International Journal of Engineering, Science and Humanities
An international peer reviewed, refereed, open-access journal
Impact Factor 8.3 www.ijesh.com ISSN: 2250-3552

# Fuzzy and Fixed-Point Methods for Modeling Uncertainty in Physical Systems

**Dr. Sumeet P Mane**
Department of Mathematics, L.B.S. Senior College, Partur-431501
**Amol M Mandpe**
Department of Physics, Vinayakrao Patil Mahavidyalaya, Vaijapur-423701

**Abstract**
Physical systems are rarely described by parameters that are known exactly. Material properties, loads and boundary conditions are measured with limited precision, and the outputs of a model inherit that imprecision. This paper examines how fuzzy set theory and fixed point methods can be combined to propagate non-probabilistic uncertainty through nonlinear equilibrium problems. A hardening spring under a vertical load is used as a representative physical system, with the load, the linear stiffness and the cubic stiffness expressed as triangular fuzzy numbers. The equilibrium equation is rewritten as a fixed point problem, a contraction condition is derived from the Lipschitz constant of the iteration map, and the fuzzy fixed point is built level by level using α-cuts and the monotonicity of the map. Picard, Mann and Ishikawa iterations are compared on nominal and extreme parameter sets, and the fuzzy solution is checked against a Monte Carlo simulation with 200,000 samples. The fuzzy equilibrium displacement has a core of 341.16 mm and a support from 276.84 mm to 406.14 mm. Mann iteration converged in 9 to 14 steps at a tolerance of $10^{-8}$, whereas Picard iteration needed 25 to 73 steps. The fuzzy support enclosed the Monte Carlo range, and the two approaches agreed on the central value within 0.6 mm. The study shows that the α-cut fixed point approach is a transparent and inexpensive alternative when only interval-type information about the parameters is available.
**Keywords:** fuzzy numbers; α-cuts; fixed point theory; contraction mapping; Mann iteration; uncertainty propagation; nonlinear equilibrium

## 1. Introduction

### 1.1 Background

Mathematical models are the main tool used to predict how physical systems behave. A bridge deflects under traffic, a rod conducts heat, a circuit settles to a steady voltage, and in each case an equation or a system of equations links the inputs of the problem to the quantity of interest. The quality of the prediction depends on the structure of the model and, just as importantly, on the numbers placed inside it. Stiffness, conductivity, damping, load and geometry are all obtained through measurement, estimation or manufacturer data, and none of them is known with infinite precision.

International Journal of Engineering, Science and Humanities
An international peer reviewed, refereed, open-access journal
Impact Factor 8.3 www.ijesh.com ISSN: 2250-3552

The consequence is that a deterministic answer, such as a single displacement of 341 mm, can give a false impression of certainty. Engineers and scientists have long recognised that a model output should be accompanied by some statement of how far it can be trusted. This realisation has produced a large body of work on uncertainty quantification, which has grown rapidly because of the need for reliable predictions in engineering design, climate science, medicine and data-driven modeling (Abdar et al., 2021; Sullivan, 2015).

**1.2 Uncertainty in Physical Modeling**

Uncertainty in physical modeling is usually divided into two types. Aleatory uncertainty is the natural variability of a quantity that would differ from one trial to the next even if everything were measured perfectly. Epistemic uncertainty, by contrast, comes from lack of knowledge and could in principle be reduced by collecting more data or building a better model (Hüllermeier & Waegeman, 2021). Many practical problems contain both, but the proportion differs greatly from case to case.

Probabilistic methods are the standard response to aleatory uncertainty, and they work well when enough data exist to fit a distribution. Their weakness appears when the information is scarce. A designer who knows only that the stiffness of a spring lies between 90 and 110 N/m, with a most likely value near 100 N/m, cannot justify a particular probability density without adding assumptions that the data do not support. Choosing a distribution in such a case can hide the true state of knowledge and produce results that look more precise than they are. Methods that carry imprecision directly, rather than converting it into probability, are therefore of practical interest (Ghanem et al., 2017).

**1.3 Fixed Point Theory in Applied Analysis**

Fixed point theory studies equations of the form $x = T(x)$, where a point is mapped to itself by an operator. The best-known result is the contraction mapping principle, which guarantees a unique solution and a constructive iterative method whenever the operator shrinks distances by a fixed factor smaller than one. Many equilibrium and steady-state problems in physics can be written in this form with little effort, because a steady state is by definition a state that no longer changes under the governing dynamics.

The theory has been widened considerably during the past decade. Generalised contractions, simulation functions and interpolative conditions have relaxed the original requirement while still ensuring existence of fixed points (Karapınar, 2018; Khojasteh et al., 2015; Roldán-López-de-Hierro et al., 2015). The same ideas have been applied to nonlinear fractional differential equations and to integral equations, which shows that the framework is relevant to equations that arise directly from physical laws (Gopal et al., 2016; Sintunavarat, 2016). A broad view of

International Journal of Engineering, Science and Humanities
An international peer reviewed, refereed, open-access journal
Impact Factor 8.3 www.ijesh.com ISSN: 2250-3552

applications in science, engineering and the behavioural sciences is given by Debnath et al. (2021).

### 1.4 Fuzzy Sets as a Model of Imprecision

Fuzzy set theory replaces the sharp yes-or-no membership of classical sets with a degree of membership between zero and one. A fuzzy number is a fuzzy set on the real line that describes a quantity such as “about 100 N/m”. Its membership function peaks at the most plausible value and falls to zero at the limits of what is considered possible. Triangular and trapezoidal shapes are common because they can be specified by three or four numbers that an expert can supply without difficulty.

A key feature of fuzzy numbers is that each of them can be decomposed into a family of nested closed intervals called α-cuts. At $\alpha = 1$ the interval collapses to the core, the most plausible value, and at $\alpha = 0$ it expands to the full support. Arithmetic and function evaluation with fuzzy numbers can therefore be carried out as interval computations at each level, which is cheap and easy to interpret. Possibility theory gives a formal account of how such graded information relates to belief and plausibility, and shows how it differs from probability (Dubois & Prade, 2015).

### 1.5 Scope and Structure of the Paper

This paper joins the two ideas described above. An equilibrium equation with fuzzy parameters is converted into a fixed-point problem, and the fuzzy solution is constructed from the fixed points of the corresponding interval problems at every α-level. The aim is not to prove a new abstract theorem but to show, with a worked physical example and complete numerical evidence, how the construction operates, when it converges, how fast different iteration schemes reach the answer, and how the result compares with a probabilistic benchmark.

The remainder of the paper is organised as follows. Section 2 reviews related work on uncertainty quantification, fixed point theory and fuzzy analysis. Section 3 presents the mathematical formulation, the physical model and the numerical procedures. Section 4 reports four tables and four figures and discusses them. Section 5 summarises the findings and indicates directions for further work.

## 2. Literature Review

### 2.1 Uncertainty Quantification in Physical Systems

Uncertainty quantification has developed into a discipline of its own. Sullivan (2015) presents the mathematical foundations of the subject, including probabilistic, interval-based and information-theoretic viewpoints, and stresses that the choice of representation should follow the nature of the available information. The Handbook of Uncertainty Quantification edited by

International Journal of Engineering, Science and Humanities
An international peer reviewed, refereed, open-access journal
Impact Factor 8.3 www.ijesh.com ISSN: 2250-3552

Ghanem et al. (2017) collects methods for forward propagation, inverse problems, sensitivity analysis and surrogate modeling, and shows that no single technique suits every application.

Recent surveys have concentrated on machine learning. Abdar et al. (2021) reviewed uncertainty quantification in deep learning and discussed techniques, applications and open challenges. Hüllermeier and Waegeman (2021) explained how aleatoric and epistemic uncertainty should be distinguished in learning problems and argued that treating them separately leads to better decisions. Although these works address data-driven models, the distinction they draw applies equally to physics-based models, where parameter imprecision is mostly epistemic and often poorly described by a probability density.

A common observation across these studies is that the cost of sampling-based propagation grows quickly when the forward model is expensive. This explains the continued interest in methods that need only a small number of model evaluations, such as interval and fuzzy arithmetic, which evaluate the model at the endpoints of α-cuts instead of at thousands of random points.

**2.2 Fixed Point Theory and Generalised Contractions**

Fixed point theory has produced many extensions of the original contraction principle. Karapınar (2018) revisited Kannan-type contractions through an interpolation technique, which replaced a linear combination of distances by a product of powers and thereby produced a new family of conditions. Karapınar et al. (2018) extended interpolative Reich–Rus–Ćirić contractions to partial metric spaces, and Aydi et al. (2019) introduced ω-interpolative conditions of the Ćirić–Reich–Rus type. Khojasteh et al. (2015) proposed simulation functions as a unifying device that covers many earlier contractive conditions, and Roldán-López-de-Hierro et al. (2015) used the same device to obtain coincidence point theorems.

A parallel line of work has relaxed the metric structure itself. Kamran et al. (2017) generalised the notion of a b-metric space, Rakić et al. (2020) proved new fixed point results in b-metric spaces, and Karapınar and Fulga (2019) introduced hybrid contractions in the same setting. Debnath and de la Sen (2019) studied set-valued interpolative contractions, and Alamgir et al. (2020) obtained results under a Hausdorff controlled type metric. The set-valued and Hausdorff-type settings are especially relevant here, because the α-cuts of a fuzzy number are sets, and the distance between two fuzzy numbers is commonly built from the Hausdorff distance between their cuts.

Applications have followed the theory. Gopal et al. (2016) used F-contractions of α-type to study a nonlinear fractional differential equation, Sintunavarat (2016) treated nonlinear integral equations in b-metric spaces, and Ali et al. (2017) obtained solutions of a Volterra integral inclusion. These examples show that fixed point arguments are routinely used to prove the existence of solutions to equations that describe physical processes. They rarely address,

International Journal of Engineering, Science and Humanities
An international peer reviewed, refereed, open-access journal
Impact Factor 8.3 www.ijesh.com ISSN: 2250-3552

however, how imprecise parameters affect the fixed point, which is the question taken up in the present study.

### 2.3 Fuzzy Numbers and Fuzzy Fixed Point Approaches

Working with fuzzy-number-valued quantities requires a notion of distance and, for dynamic problems, a notion of derivative. Mazandarani et al. (2018) introduced granular differentiability for fuzzy-number-valued functions, which overcomes some of the difficulties of earlier definitions, such as the growth of the support width with time. Dubois and Prade (2015) reviewed possibility theory and described how fuzzy sets relate to uncertainty modeling, with attention to the meaning of the degrees of membership.

The metric fixed point literature supplies the structure needed for a fixed point argument on spaces of fuzzy numbers. The book of Debnath et al. (2021) places metric fixed point theory beside applications in several fields and shows that complete metric spaces of sets or functions are a natural setting for such arguments. When the distance between fuzzy numbers is defined as the supremum of the Hausdorff distances between α-cuts, completeness of the space of fuzzy numbers allows the contraction principle to be applied level by level.

Two gaps can be identified in the existing material. First, studies of generalised contractions usually concentrate on existence and uniqueness, with limited attention to the numerical behaviour of the iterations on a concrete physical problem. Second, work on fuzzy modeling in physics seldom uses the iteration form of the equilibrium equation, even though this form gives a direct measure of convergence through the Lipschitz constant. The present paper addresses both points with a single worked example.

## 3. Research Methodology

### 3.1 Fuzzy Preliminaries

Let X be the real line and let A be a fuzzy subset of X with membership function μ from X to the interval [0, 1]. The α-cut of A is the crisp set of all points whose degree of membership is at least α. For a fuzzy number the α-cuts are closed bounded intervals, and they are nested, so that a larger α gives a smaller interval. The α-cut is defined by Equation 1.

$$[A]^{\alpha} = \{, x \in X : \mu_A(x) \geq \alpha\}, \quad \alpha \in (0, 1] \tag{1}$$

A fuzzy number is called triangular when it is specified by three numbers $a \leq m \leq b$, where a and b are the lower and upper limits of the support and m is the modal value. Its membership function is given by Equation 2, and its α-cut is the interval $[a + \alpha(m - a), b - \alpha(b - m)]$.

$$\mu(x) = \max(, 0, \min(, \frac{x - a}{m - a}, \frac{b - x}{b - m})) \tag{2}$$

When a function of fuzzy arguments is needed, the extension principle gives the membership function of the result. For a function f applied to a fuzzy set A, the membership degree of a value

International Journal of Engineering, Science and Humanities
An international peer reviewed, refereed, open-access journal
Impact Factor 8.3 www.ijesh.com ISSN: 2250-3552

y is the highest membership degree among all arguments that f maps to y, as stated in Equation 3.

$$\mu_{f(A)}(y) = \sup_{x:\, f(x)=y} \mu_A(x) \quad (3)$$

For continuous and monotone functions, the extension principle is equivalent to applying f to the α-cuts, and the image of each α-cut is the α-cut of the image. This equivalence is used throughout the paper because it reduces a fuzzy computation to a sequence of interval computations. To measure the distance between two fuzzy numbers u and v, the supremum metric of Equation 4 is used, where d with subscript H denotes the Hausdorff distance between two intervals.

$$d_\infty(,u,v) = \sup_{\alpha \in [0,1]} d_H(,[u]^\alpha,[v]^\alpha) \quad (4)$$

Under this metric the space of fuzzy numbers is complete, so the contraction principle can be stated for operators acting on it. In the present study the operator acts on real numbers at each α-level, and the metric of Equation 4 is used only to compare fuzzy results with one another.

**3.2 Physical Model**

The physical system is a hardening spring that supports a vertical load F. The spring is stiffer than a linear spring at large displacements, which is typical of rubber mounts, cables and thin plates under membrane action. Its restoring force is the sum of a linear term with stiffness k and a cubic term with stiffness c. The static equilibrium displacement x is the point at which the restoring force balances the load, as written in Equation 5.

This equation has no closed form that is convenient for repeated evaluation under varying parameters, but it is well suited to iterative solution. Because the restoring force is strictly increasing in x and equals zero at x = 0, a unique positive solution exists for every positive F, k and c. This existence argument does not require fixed point theory. The fixed point formulation is introduced because it gives an explicit convergence measure and a family of simple iterative algorithms.

$$k\,x + c\,x^3 = F \quad (5)$$

Solving Equation 5 for the linear term gives the fixed point form shown in Equation 6, where T is the iteration map. The map is positive, decreasing in x, increasing in F and decreasing in k and c.

$$x = T(x) = \frac{F}{k + c\,x^2} \quad (6)$$

Three parameters of the model are treated as triangular fuzzy numbers: the load F, the linear stiffness k and the cubic stiffness c. Their supports and modal values are listed in Table 1 in Section 4. The quantity of interest is the fuzzy equilibrium displacement x*, whose membership function is to be determined.

International Journal of Engineering, Science and Humanities
An international peer reviewed, refereed, open-access journal
Impact Factor 8.3 www.ijesh.com ISSN: 2250-3552

### 3.3 Fuzzy Fixed Point Formulation

For crisp parameters the contraction mapping principle applies on any interval where the map T has a Lipschitz constant below one. The condition for contraction is given in Equation 7. If it holds, the sequence generated by repeated application of T converges to the unique fixed point from every starting point in the interval.

$$|T(x) - T(y)| \leq L\,|x - y|, \quad 0 \leq L < 1 \tag{7}$$

When the contraction condition holds, the distance between an iterate and the fixed point is bounded in terms of the first step of the iteration. This a priori estimate is given by Equation 8 and is used to decide how many iterations are needed for a prescribed accuracy.

$$|x_n - x^*| \leq \frac{L^n}{1-L}\,|x_1 - x_0| \tag{8}$$

For the spring model the derivative of T at the fixed point can be evaluated explicitly. Using $T(x^*) = x^*$, the Lipschitz constant takes the form of Equation 9. This constant is smaller than one precisely when $c(x^*)^2 < k$, that is, when the cubic part of the restoring force is smaller than the linear part at equilibrium. The condition is a local one, and it holds in a neighbourhood of the fixed point.

$$L = |T'(x^*)| = \frac{2\,c\,(x^*)^2}{k + c\,(x^*)^2} \tag{9}$$

The fuzzy problem is solved level by level. Because the restoring force is increasing in x, the solution x* increases with the load F and decreases with each of the stiffnesses k and c. The smallest displacement at level α is therefore obtained by pairing the lowest load with the highest stiffnesses, and the largest displacement by pairing the highest load with the lowest stiffnesses. Denoting the lower and upper endpoints of the α-cuts of the parameters by the subscripts L and U, the α-cut of the fuzzy fixed point is given by Equation 10. The lower endpoint is the fixed point of T evaluated at the lowest load and the highest stiffnesses, and the upper endpoint is the fixed point of T evaluated at the highest load and the lowest stiffnesses.

$$[x^*]^\alpha = [, x_L(\alpha), x_U(\alpha)], \quad x_L(\alpha) = T(x_L(\alpha);\, F_L(\alpha), k_U(\alpha), c_U(\alpha)) \tag{10}$$

Since x* is a continuous and monotone function of each parameter, the extension principle of Equation 3 guarantees that the intervals in Equation 10 are exactly the α-cuts of the fuzzy equilibrium displacement. No search over interior parameter combinations is needed, and each α-level requires only two fixed point computations. For a grid of n levels the total cost is 2n small iterative solutions.

### 3.4 Iterative Schemes

Three iteration schemes are compared. The Picard iteration applies the map directly, so that each new point is the image of the previous one. This scheme is the one that appears in the contraction mapping principle. The Mann iteration uses a convex combination of the current point and its

International Journal of Engineering, Science and Humanities
An international peer reviewed, refereed, open-access journal
Impact Factor 8.3 www.ijesh.com ISSN: 2250-3552

image, with a constant weight λ between zero and one, as given by Equation 11. The Ishikawa iteration adds a second averaging step: an intermediate point y is first computed as a combination of the current point and its image with weight β, and the new point is then formed from the current point and the image of y with weight α. In this study λ = α = β = 0.5 is used.

The reason for expecting Mann and Ishikawa schemes to converge faster here is the sign of the derivative. Because T is a decreasing map, its derivative at the fixed point is negative and the Picard iterates alternate around the solution. Averaging with the previous iterate damps this oscillation. With λ = 0.5, the local error factor of the Mann scheme is $|1 - \lambda + \lambda T'(x^*)|$, which is smaller than the Picard factor $|T'(x^*)|$ whenever $T'(x^*)$ is negative and the map is a contraction of moderate strength.

$$x_{n+1} = (1 - \lambda)\, x_n + \lambda\, T(x_n) \tag{11}$$

All three schemes are started from $x_0 = 0$ and stopped when the absolute difference between successive iterates falls below $10^{-8}$. The number of iterations needed to reach this tolerance is the measure of speed that is reported.

**3.5 Numerical Experiment and Validation**

The parameter values were chosen to represent a small mechanical mount: a nominal load of 50 N with a spread of ±20%, a linear stiffness of 100 N/m with ±10%, and a cubic stiffness of 400 N/m³ with ±12.5%. The experiment was carried out in Python with double-precision arithmetic. The α-levels used in the main tables are 0, 0.25, 0.5, 0.75 and 1, and a finer grid of 201 levels was used for the figures.

Two checks were applied to the fuzzy solution. First, every endpoint reported in Table 2 was compared with the real root of the cubic polynomial in Equation 5, found by an independent root-finding routine, and the two values agreed to within $10^{-6}$ m. Second, the fuzzy solution was compared with a Monte Carlo simulation in which the three parameters were drawn independently from triangular probability distributions with the same supports and modes as the fuzzy numbers, and the equilibrium displacement was computed for 200,000 samples. The Monte Carlo benchmark is not a competing truth. It answers a different question, since it assumes independence and a specific distribution, but it is a useful reference for the width and position of the fuzzy result.

The centroid of the fuzzy solution was used as a defuzzified value. Using the identity that expresses the membership function as an integral of the indicator functions of its α-cuts, the centroid can be computed from the endpoints directly, as shown in Equation 12.

$$x_c = \frac{\int_{,0}^{1} \frac{1}{2} (x_U{}^2(\alpha) - x_L{}^2(\alpha))\, d\alpha}{\int_{,0}^{1} (x_U(\alpha) - x_L(\alpha))\, d\alpha} \tag{12}$$

International Journal of Engineering, Science and Humanities
An international peer reviewed, refereed, open-access journal
Impact Factor 8.3 www.ijesh.com ISSN: 2250-3552

The integrals were evaluated by the trapezoidal rule on the fine α-grid. Sensitivity of the width of the fuzzy solution to each parameter was examined by fuzzifying one parameter at a time while keeping the others at their modal values.

## 4. Results and Discussion

This section reports the outcome of the numerical experiment described in Section 3.5. All displacements are given in millimetres. The results are organised in four parts: the fuzzy parameters and the resulting fuzzy solution, the behaviour of the iterative schemes, the sensitivity to individual parameters, and the comparison with Monte Carlo simulation. The figures and tables are generated from the computations and were not adjusted by hand.

### 4.1 Fuzzy Input Parameters

Table 1 lists the three triangular fuzzy parameters. The load carries the largest relative spread, ±20% of its modal value, followed by the cubic stiffness at ±12.5% and the linear stiffness at ±10%. These spreads are representative of the imprecision in a typical laboratory or catalogue specification and were chosen so that the three parameters contribute at different levels to the output uncertainty.

**Table 1**

Triangular fuzzy parameters of the nonlinear spring model

| Parameter | Lower (a) | Modal (m) | Upper (b) | Unit |
|---|---|---|---|---|
| Load, F | 40.0 | 50.0 | 60.0 | N |
| Linear stiffness, k | 90.0 | 100.0 | 110.0 | N/m |
| Cubic stiffness, c | 350.0 | 400.0 | 450.0 | N/m³ |

Note. All three parameters are ±20% (F), ±10% (k) and ±12.5% (c) around the modal value.

### 4.2 Fuzzy Equilibrium Displacement

Table 2 gives the α-cuts of the fuzzy equilibrium displacement for five levels. At $\alpha = 1$ the interval collapses to a single value of 341.16 mm, which is the equilibrium of the nominal spring, and this value satisfies Equation 5 exactly to the precision of the computation: $100 \times 0.34116 + 400 \times 0.34116^3$ equals 50.0 N. At $\alpha = 0$ the interval extends from 276.84 mm to 406.14 mm, so the full support has a width of 129.30 mm. This is 37.9% of the nominal displacement, which is larger than any of the individual parameter spreads, because the three imprecise parameters act in the same direction when the extreme combinations are used.

**Table 2**

α-cuts of the fuzzy equilibrium displacement x* (mm)

| α | Lower end | Upper end | Width | Midpoint |
|---|---|---|---|---|
| 0.00 | 276.84 | 406.14 | 129.30 | 341.49 |
| 0.25 | 292.99 | 389.70 | 96.71 | 341.34 |

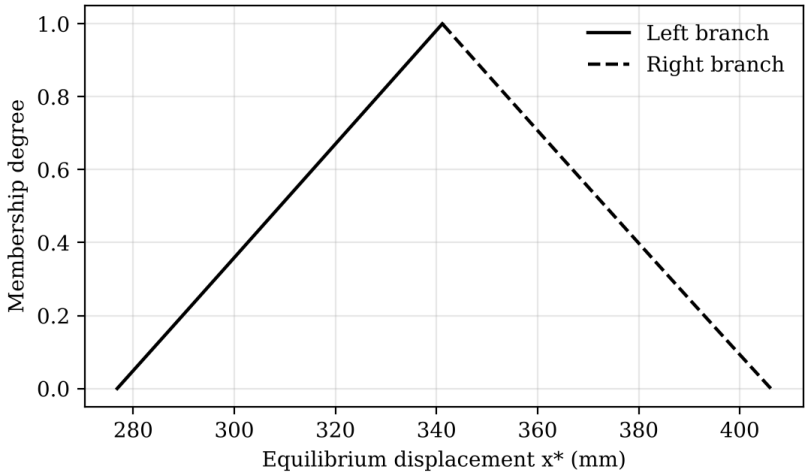
International Journal of Engineering, Science and Humanities
An international peer reviewed, refereed, open-access journal
Impact Factor 8.3 www.ijesh.com ISSN: 2250-3552

| | | | | |
|---|---|---|---|---|
| 0.50 | 309.07 | 373.41 | 64.34 | 341.24 |
| 0.75 | 325.12 | 357.25 | 32.13 | 341.18 |
| 1.00 | 341.16 | 341.16 | 0.00 | 341.16 |

Note. Endpoints were obtained from Equation 10 with Mann iteration (tolerance $10^{-8}$) and checked against the cubic roots.

**Figure 1**

Membership function of the fuzzy equilibrium displacement




Note. Solid and dashed curves are the left and right branches of the membership function obtained from the α-cuts.

Figure 1 shows the resulting membership function. It is close to triangular but not exactly so. The distance from the core to the lower limit is 64.32 mm, while the distance to the upper limit is 64.98 mm, so the shape is slightly skewed towards larger displacements. The skewness is also visible in the midpoints in Table 2, which rise from 341.16 mm at α = 1 to 341.49 mm at α = 0. The shift of 0.33 mm is small, but it shows that the nonlinearity of the model slightly distorts the triangular shape of the inputs. The width of the α-cuts decreases almost linearly with α, from 129.30 mm at α = 0 to 64.34 mm at α = 0.5 and 32.13 mm at α = 0.75. A purely linear model would produce an exactly triangular output, so the deviation from linearity in this example is mild.

### 4.3 Convergence of the Iterative Schemes

Table 3 compares the three iteration schemes on the nominal parameters and on the two extreme parameter sets at α = 0. The Lipschitz constant from Equation 9 is below one in all three cases, being 0.635 for the nominal set, 0.477 for the set that gives the smallest displacement and 0.782 for the set that gives the largest displacement. The contraction condition is therefore satisfied

International Journal of Engineering, Science and Humanities
An international peer reviewed, refereed, open-access journal
Impact Factor 8.3 www.ijesh.com ISSN: 2250-3552

everywhere that matters for the fuzzy construction, and the Picard iteration converges in each case. The size of the constant explains the Picard iteration counts: 25 steps are needed when L is 0.477, 40 steps when L is 0.635, and 73 steps when L is 0.782. The count grows as the constant approaches one, as would be expected from the a priori estimate of Equation 8.

**Table 3**

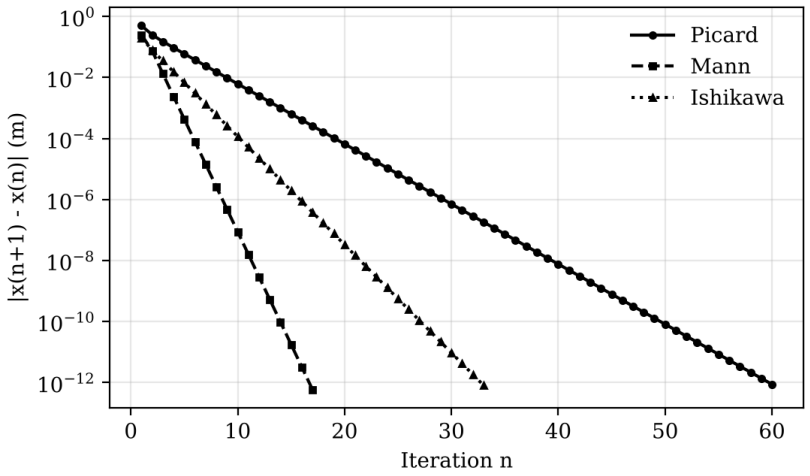
Lipschitz constants and iteration counts for three parameter sets

| Parameter set | L | Picard | Mann | Ishikawa |
|---|---|---|---|---|
| Nominal ($\alpha = 1$) | 0.635 | 40 | 12 | 22 |
| Lower bound ($\alpha = 0$) | 0.477 | 25 | 14 | 21 |
| Upper bound ($\alpha = 0$) | 0.782 | 73 | 9 | 23 |

Note. Starting point $x_0 = 0$, stopping rule $|x_{n+1} - x_n| < 10^{-8}$, $\lambda = 0.5$ for Mann, and $\alpha = \beta = 0.5$ for Ishikawa.

**Figure 2**

Convergence of the three iterative schemes for the nominal parameters




Note. The vertical axis is logarithmic; Picard, Mann and Ishikawa iterations start from $x_0 = 0$.

The Mann scheme needed 12, 14 and 9 steps for the same three cases. It is faster than Picard in every case, and its advantage is largest at the upper bound, where Picard is slowest. At that point the local error factor of the Mann scheme is $|0.5 - 0.5 \times 0.782| = 0.109$, compared with 0.782 for Picard, which agrees with the observed reduction from 73 to 9 steps. The Ishikawa scheme needed 22, 21 and 23 steps, which places it between the two others and makes it almost insensitive to the choice of parameter set.

Figure 2 shows the same behaviour for the nominal parameters. The Picard error falls steadily but slowly. The Mann error drops more quickly, and the Ishikawa error lies between them. All

International Journal of Engineering, Science and Humanities
An international peer reviewed, refereed, open-access journal
Impact Factor 8.3 www.ijesh.com ISSN: 2250-3552

three curves are straight lines on the logarithmic scale, which is the signature of linear convergence and confirms that the contraction analysis describes the iterations correctly. One practical consequence is that for the fuzzy construction the Mann scheme is the better choice, since the endpoints that require the most work are those with the largest Lipschitz constant.

**4.4 Sensitivity and Comparison with Monte Carlo Simulation**

Figure 3 shows how the width of the α-cut depends on α when all three parameters are fuzzy and when each is fuzzy on its own. At α = 0, the load alone produces a width of 84.06 mm, the linear stiffness alone produces 28.46 mm, and the cubic stiffness alone produces 16.64 mm. These three values add up to 129.16 mm, which is within 0.2 mm of the width obtained when all parameters are fuzzy together (129.30 mm). The near-additivity indicates that interactions between the parameters are weak over the ranges considered. The load is clearly the dominant source of imprecision, and reducing its spread would give the largest improvement in the precision of the result. This kind of conclusion is available directly from the α-cut construction, without any additional sampling.

Table 4 and Figure 4 compare the fuzzy solution with the Monte Carlo simulation. The Monte Carlo mean of 340.72 mm differs from the fuzzy core of 341.16 mm by 0.44 mm and from the fuzzy centroid of 341.32 mm by 0.60 mm, which is less than 0.2% of the displacement. The Monte Carlo standard deviation is 18.37 mm. The full Monte Carlo range, from 282.19 mm to 398.21 mm, lies inside the fuzzy support, from 276.84 mm to 406.14 mm. This is expected, since the fuzzy support corresponds to the simultaneous occurrence of all three extreme parameter values, which has very small probability and is almost never sampled. The fuzzy support is 11.4% wider than the Monte Carlo range, and its width of 129.30 mm compares with 116.02 mm.

**Table 4**

Comparison of the fuzzy α-cut solution with Monte Carlo simulation (mm)

| Quantity | Fuzzy (α-cut) | Monte Carlo |
|---|---|---|
| Central value (core / mean) | 341.16 | 340.72 |
| Centroid of fuzzy solution | 341.32 | — |
| Standard deviation | — | 18.37 |
| Full range, lower (α = 0 / minimum) | 276.84 | 282.19 |
| Full range, upper (α = 0 / maximum) | 406.14 | 398.21 |
| Full range, width | 129.30 | 116.02 |
| Mid interval, lower (α = 0.5 / 5th percentile) | 309.07 | 309.54 |
| Mid interval, upper (α = 0.5 / 95th | 373.41 | 370.58 |

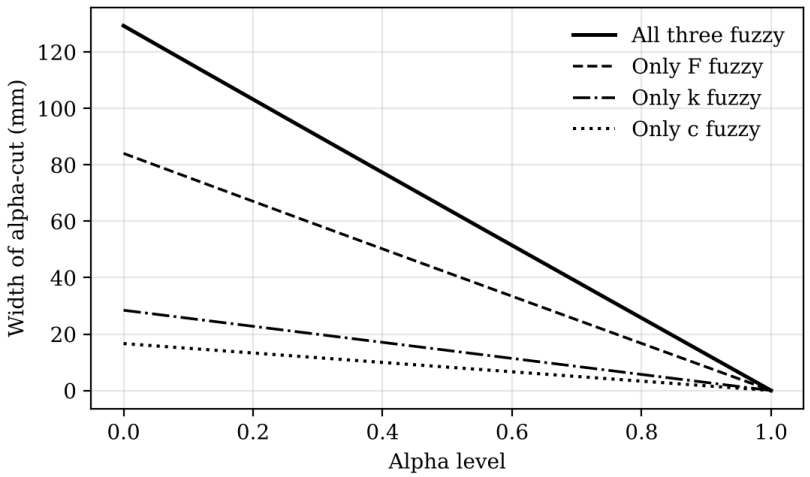
International Journal of Engineering, Science and Humanities
An international peer reviewed, refereed, open-access journal
Impact Factor 8.3 www.ijesh.com ISSN: 2250-3552

| | | |
|---|---|---|
| percentile) | | |
| Mid interval, width | 64.34 | 61.04 |

Note. Monte Carlo used 200,000 samples with triangular distributions on the same supports as the fuzzy parameters.

**Figure 3**

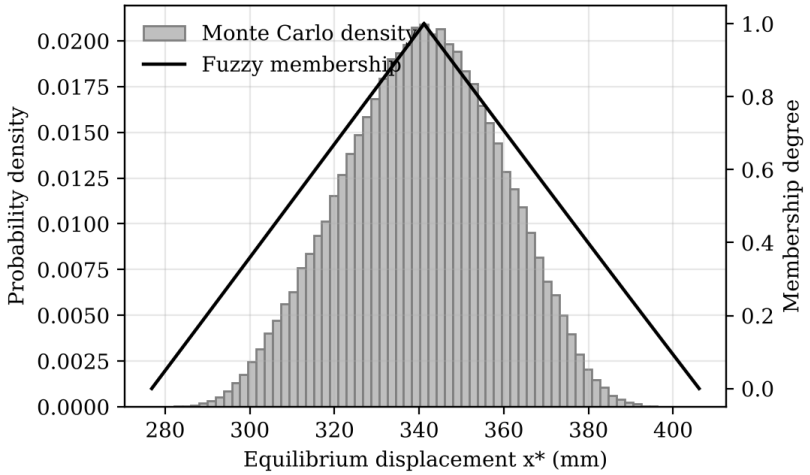
Width of the α-cut of the fuzzy fixed point against α




Note. Curves show the effect of fuzzifying all three parameters together and each parameter alone.

**Figure 4**

Monte Carlo density compared with the fuzzy membership function




Note. The histogram uses the left axis; the membership curves use the right axis.

International Journal of Engineering, Science and Humanities
An international peer reviewed, refereed, open-access journal
Impact Factor 8.3 www.ijesh.com ISSN: 2250-3552

A closer correspondence appears at the middle of the distribution. The $\alpha = 0.5$ interval, from 309.07 mm to 373.41 mm, is close to the interval between the 5th and 95th percentiles of the Monte Carlo sample, from 309.54 mm to 370.58 mm. The widths are 64.34 mm and 61.04 mm. In Figure 4 the histogram and the membership function are centred at the same place, but the histogram is concentrated near the centre while the membership function decreases linearly towards the limits. The two curves answer different questions and should not be expected to coincide. The membership function reports which displacements are compatible with the specified parameter ranges, whereas the histogram reports how often each displacement would occur under an assumed joint distribution.

Three points of discussion follow from these results. First, the α-cut fixed point method required only 10 fixed point solutions to produce Table 2 (two for each of five levels), and 402 solutions for the fine grid, while the Monte Carlo benchmark needed 200,000. Since each fixed point solution takes only a few iterations, the fuzzy approach is much cheaper, and the saving would be larger for a model that is expensive to evaluate. Second, the fuzzy interval is conservative with respect to the sampling-based range, which is a desirable property in design, although it may be pessimistic when the parameters are in fact independent. Third, the construction used here depends on monotonicity of the solution with respect to each parameter. This holds for the spring model, but it cannot be assumed for every physical system, and for non-monotone problems an optimisation step at each α-level would be needed to find the endpoints.

The study has limitations that should be stated plainly. The model has a single unknown and three uncertain parameters, so the example illustrates the method but does not demonstrate performance on high-dimensional problems. The contraction condition was verified through the Lipschitz constant at the fixed point and confirmed by the observed convergence, and not proved globally over an interval. Finally, the Monte Carlo reference rests on a triangular distribution with independent parameters, and different assumptions would shift the comparison.

## 5. Conclusion

This paper combined fuzzy set theory with fixed point methods to study how imprecise parameters affect the equilibrium of a nonlinear physical system. The equilibrium equation of a hardening spring was written as a fixed point problem, and the fuzzy equilibrium displacement was constructed from the fixed points of interval problems at each α-level. Because the solution is monotone in each parameter, the endpoints of every α-cut follow from two crisp fixed point computations at suitably chosen parameter combinations.

The numerical results support three conclusions. The fuzzy displacement has a core of 341.16 mm and a support from 276.84 mm to 406.14 mm, and its membership function is nearly triangular with a slight skew towards larger displacements. The contraction condition, expressed

International Journal of Engineering, Science and Humanities
An international peer reviewed, refereed, open-access journal
Impact Factor 8.3 www.ijesh.com ISSN: 2250-3552

through the Lipschitz constant $2c(x^*)^2/(k + c(x^*)^2)$, was satisfied for all parameter sets, with values from 0.477 to 0.782, and Mann iteration converged in 9 to 14 steps against 25 to 73 steps for the Picard iteration. The comparison with 200,000 Monte Carlo samples showed agreement on the central value within 0.6 mm and a conservative fuzzy support that enclosed the sampled range.

The approach offers a practical route to uncertainty propagation when only ranges and most likely values are known, and it provides a direct reading of parameter importance through the α-cut widths. Future work can proceed in three directions: extending the construction to systems of equations and to differential equations through the metric fixed point results reviewed in Section 2, treating non-monotone problems through optimisation at each α-level, and combining fuzzy and probabilistic descriptions in a single model for problems that contain both epistemic and aleatory uncertainty.

**REFERENCES**

1. Abdar, M., Pourpanah, F., Hussain, S., Rezazadegan, D., Liu, L., Ghavamzadeh, M., Fieguth, P., Cao, X., Khosravi, A., Acharya, U. R., Makarenkov, V., & Nahavandi, S. (2021). A review of uncertainty quantification in deep learning: Techniques, applications and challenges. Information Fusion, 76, 243–297.
2. Alamgir, N., Kiran, Q., Işık, H., & Aydi, H. (2020). Fixed point results via a Hausdorff controlled type metric. Advances in Difference Equations, 2020, Article 24.
3. Ali, M. U., Kamran, T., & Postolache, M. (2017). Solution of Volterra integral inclusion in b-metric spaces via new fixed point theorem. Nonlinear Analysis: Modelling and Control, 22(1), 17–30.
4. Aydi, H., Karapınar, E., & Roldán López de Hierro, A. F. (2019). ω-interpolative Ćirić–Reich–Rus-type contractions. Mathematics, 7(1), Article 57.
5. Debnath, P., & de la Sen, M. (2019). Set-valued interpolative Hardy–Rogers and set-valued Reich–Rus–Ćirić-type contractions in b-metric spaces. Mathematics, 7(9), Article 849.
6. Debnath, P., Konwar, N., & Radenović, S. (2021). Metric fixed point theory: Applications in science, engineering and behavioural sciences. Springer.
7. Dubois, D., & Prade, H. (2015). Possibility theory and its applications: Where do we stand? In J. Kacprzyk & W. Pedrycz (Eds.), Springer handbook of computational intelligence (pp. 31–60). Springer.
8. Ghanem, R., Higdon, D., & Owhadi, H. (Eds.). (2017). Handbook of uncertainty quantification. Springer.

9. Gopal, D., Abbas, M., Patel, D. K., & Vetro, C. (2016). Fixed points of α-type F-contractive mappings with an application to nonlinear fractional differential equation. Acta Mathematica Scientia, 36(3), 957–970.
10. Hüllermeier, E., & Waegeman, W. (2021). Aleatoric and epistemic uncertainty in machine learning: An introduction to concepts and methods. Machine Learning, 110(3), 457–506.
11. Kamran, T., Samreen, M., & Ain, Q. U. (2017). A generalization of b-metric space and some fixed point theorems. Mathematics, 5(2), Article 19.
12. Karapınar, E. (2018). Revisiting the Kannan type contractions via interpolation. Advances in the Theory of Nonlinear Analysis and Its Application, 2(2), 85–87.
13. Karapınar, E., Agarwal, R., & Aydi, H. (2018). Interpolative Reich–Rus–Ćirić type contractions on partial metric spaces. Mathematics, 6(11), Article 256.
14. Karapınar, E., & Fulga, A. (2019). New hybrid contractions on b-metric spaces. Mathematics, 7(7), Article 578.
15. Khojasteh, F., Shukla, S., & Radenović, S. (2015). A new approach to the study of fixed point theory for simulation functions. Filomat, 29(6), 1189–1194.
16. Mazandarani, M., Pariz, N., & Kamyad, A. V. (2018). Granular differentiability of fuzzy-number-valued functions. IEEE Transactions on Fuzzy Systems, 26(1), 310–323.
17. Rakić, D., Mukheimer, A., Došenović, T., Mitrović, Z. D., & Radenović, S. (2020). On some new fixed point results in b-metric spaces. Journal of Inequalities and Applications, 2020, Article 99.
18. Roldán-López-de-Hierro, A. F., Karapınar, E., Roldán-López-de-Hierro, C., & Martínez-Moreno, J. (2015). Coincidence point theorems on metric spaces via simulation functions. Journal of Computational and Applied Mathematics, 275, 345–355.
19. Sintunavarat, W. (2016). Nonlinear integral equations with new admissibility types in b-metric spaces. Journal of Fixed Point Theory and Applications, 18(2), 397–416.
20. Sullivan, T. J. (2015). Introduction to uncertainty quantification. Springer.